Abnormal neurite orientation dispersion and density imaging of white matter in children with primary nocturnal enuresis

Hongbin Sun[a,*], Bing Xue[b], Miao Peng[c], Hongwei Ma[d], Bing Yu[b], Yang Hou[b], Qiyong Guo[b]

[a] Department of Radiology, The Fourth Affiliated Hospital of China Medical University, Shenyang 110032, China
[b] Department of Radiology, Shengjing Hospital of China Medical University, Shenyang 110004, China
[c] Department of Psychology, Shengjing Hospital of China Medical University, Shenyang 110004, China
[d] Department of Developmental Pediatrics, Shengjing Hospital of China Medical University, Shenyang 110004, China

ARTICLE INFO

ABSTRACT

Several lines of evidence indicate that multiple abnormalities of gray matter are related to the pathogenesis of primary nocturnal enuresis (PNE); however, few studies have been conducted with respect to abnormalities in white matter (WM) of children with PNE. The present work investigated the microstructure of WM in children with PNE using a neurite orientation dispersion and density imaging (NODDI) method. NODDI data were obtained from 29 children with PNE (age = 9.8 ± 1.2 years, 59% males) and 34 healthy controls (age = 10.3 ± 1.6 years, 56% males) in this study. Multi-b-value diffusion-weighted imaging data were acquired with a 3 T MR system, and the orientation dispersion index (ODI) and neurite density index (NDI) maps were calculated. Tract-Based Spatial Statistics analyses of WM tracts were performed with ODI and NDI maps in children with PNE and controls. Children with PNE had lower ODIs in WM fiber tracts of the bilateral superior longitudinal fasciculus (SLF) and higher ODIs in the bilateral internal capsule (IC) and right anterior thalamic radiation (ATR) than controls. PNE children also had lower NDIs in the bilateral IC and the cingulum and higher NDIs in the bilateral SLF. These changes in NODDI indices, which indicated abnormal neural maturation of the WM microstructures, may be related to abnormal sleep and enuresis in children with PNE.

1. Introduction

Primary nocturnal enuresis (PNE) is common in childhood and affects up to 15% of children. PNE causes significant psychosocial impairment in pediatric patients and is a source of frustration for their parents.

A series of imaging studies have reported multiple neural abnormalities in children with PNE during recent decades. These studies have revealed several structural, functional, and metabolic abnormalities in multiple different gray matter regions in children with PNE, including the prefrontal cortex, anterior cingulate cortex, insula, parietal lobule, pons, and thalamus (Lei et al., 2012a, 2012b, 2012c, 2015; Wang et al., 2015; Yu et al., 2011, 2012, 2013). However, fewer studies have revealed abnormalities of white matter in PNE children, and the results were not consistent. Lei et al.'s DTI study found increased mean diffusivity in the right sublobar/extranuclear white matter (WM); Yu et al.'s preliminary study discovered decreased fractional anisotropy (FA) values in WM fiber tracts of the pericallosal frontal region, the anterior limb of the internal capsule, and the middle cerebellar peduncle (Yu

et al., 2010). Therefore, further neuroimaging investigations that focus on WM fiber using more powerful techniques may be needed in PNE children.

Zhang et al. recently proposed an orientation-dispersed cylinder model of the brain microstructure to relate diffusion-weighted images, which is referred to as neurite orientation dispersion and density imaging (NODDI) (Zhang et al., 2012). The NODDI model can calculate the non-collinear properties of the neurite orientation dispersion index (ODI, corresponding to the degree of variability in fiber orientations) and the neurite density index (NDI, corresponding to the intracellular volume fraction) within each imaging voxel. This new technology has been successfully applied to evaluate pathological changes (Billiet et al., 2014) and the development of WM (Jelescu et al., 2015). It has been demonstrated that the parameters of NODDI (NDI and ODI) are able to describe the microstructure of WM tracts (Genc et al., 2017).

Because multi-shell diffusion data with multiple gradient direction acquisitions are needed to estimate the NODDI parameters, it is sometimes difficult for children to remain still during the NODDI data acquisition. Fortunately, the multi-band MRI imaging acquisition

technique has made the scan time shorter, and elevated the success rate of NODDI scans for children (Xu et al., 2013).

The objective of the present study was to detect the microstructural abnormalities of WM tracts in children with PNE using NODDI technology.

2. Methods and materials

2.1. Subjects

Thirty-five children with PNE (age range, 9.3–13.0 years; median age, 11.2 years) and 39 healthy controls (age range, 9.2–13.3 years; median age, 10.9 years) were randomly recruited for this prospective study.

The protocol used for the current study was approved by the Ethical Committee of Shengjing Hospital of China Medical University (Shenyang, China). The study procedures were explained to all parents or legal guardians of the participants and written informed consent was signed in accordance with the institutional guidelines prior to study participation.

The following inclusion criteria were used: righted-handed; age from 8 to 14 years; urination under control during the daytime; involuntary urination during sleep no less than once a month for > 3 months; and has never achieved an asymptomatic period (≥ 6 months) of consistent nighttime dryness (International Children's Continence Society). The exclusion criteria included abnormal blood and urine biochemistry; abnormal urine culture and flowmetry; kidney or urinary tract defects detected by ultrasound examination; and current diagnosis or a history of neurologic disorders or abnormalities (Nevéus et al., 2006). Children diagnosed with any neurological or psychiatric disease or with a full intelligence quotient (FIQ) scoring less than 85 were also excluded from the study.

The verbal intelligence quotient (VIQ), performance intelligence quotient (PIQ), and FIQ of each study participant were measured by trained professional staff using the China-Wechsler Intelligence Scale for Children, revised by Gong and Cai at Hunan Medical University.

Each participant completed the Childhood Behavior Checklist and underwent a Structured Clinical Interview for DSM-IV (SCID) exam performed by a qualified child psychiatrist to exclude attention-deficit/hyperactivity disorder (ADHD), conduct disorder, oppositional defiant disorder, Tourette's disorder, and any other Axis I or Axis II comorbid psychiatric disorder.

All participants underwent a routine MRI examination of the head. Their routine T1WI and T2WI brain images were inspected by a qualified neuroradiologist independent from the research project, and no structural abnormalities were found.

In all participants, a qualified nurse questioned the parents about sleep arousal at the same visit. To quantitatively evaluate arousal from sleep (AS), a questionnaire was developed according to the methodology of Chandra et al. (Chandra et al., 2004) (see **Supplementary material** for criteria of the AS scoring system). The AS scores reflect the methods parents generally use to awaken a participant to take him/her to the toilet. If AS scores varied at different hours of the night or from night to night, the highest AS score provided by the parent was used.

2.2. NODDI data acquisition

NODDI data acquisition was performed on a 3.0-T MR scanner (Ingenia; Philips Medical Systems, Best, The Netherlands) with a 32-channel radio frequency head coil. NODDI data were acquired using a multi-shell, single-shot spin-echo echo planar imaging sequence with multi-band SENSE technology in contiguous axial planes covering the entire brain. The scanning plane paralleled the anterior commissure-posterior commissure line. A thick ear cushion was used to minimize head motion during MRI scans.

Imaging parameters were set to the following values: repetition time = 4000 ms; echo time = 90 ms; number of signal acquisitions = 1; b-value = 700 and 2000 s/mm^2; diffusion sensitizing gradients = 32; parallel imaging acceleration factor = 2.5; multi-band SENSE factor = 2; slice thickness = 2 mm; slice number = 54; field of view = 224 × 224 mm; matrix = 112 × 112; and spatial resolution = 2 × 2 × 2 mm^3. Additionally, seven b0 images were acquired during NODDI data acquisition for further calculation of diffusion parameters. The total acquisition time of NODDI images was 8 min.

2.3. Image postprocessing

All NODDI images were first visually inspected after scanning. The data with obvious eddy-current distortion or motion artifacts were discarded. After visual inspection the NODDI images were preprocessed using FSL software (http://www.fmrib.ox.ac.uk/fsl). The additional pairs of b0 images acquired using reversed phase-encode directions were enrolled to estimate and correct the susceptibility-induced off-resonance field using topup tools. The resulting images were then processed using the eddy toolbox to correct eddy current-induced distortion and motion artifacts. The corrected images were then skull-stripped using BET tools of FSL.

The skull-stripped images were then processed using NODDI MATLAB toolbox software (v1.0; Microstructure Imaging Group, University College London, London, UK) to calculate the NODDI parameters (Zhang et al., 2012). The ODI and NDI maps were calculated for further analysis.

From one shell of the pre-processed NODDI data (b = 700 s/mm^2; 32 directions), FA was estimated using dtifit tools in FSL for all participants. The FA images were then normalized to the Montreal Neurological Institute space using the FMRIB Non-linear Registration Tool. The normalized FA maps for all participants were post-processed using the Tract-Based Spatial Statistics (TBSS) tool to obtain a mean FA skeleton (Smith et al., 2006). The former calculated NODDI parameter maps were normalized and projected onto the mean FA skeleton using the TBSS tool.

2.4. Statistical analysis

SPSS 17.0 software (SPSS Inc., Chicago, IL, USA) was used to perform statistical analysis. Assumptions for normality were checked using the Kolmogorov-Smirnov test for continuous data. Continuous data with a normal distribution are expressed as mean plus standard deviation (SD), and continuous data without a normal distribution are expressed as median with interquartile range.

Demographic parameters were compared between PNE and control groups using the Student's t-test or the Mann-Whitney U test, depending on the normality and homoscedasticity. The chi-square test was used to compare the sex proportion between groups. A two-tailed α-level of less than 0.05 was considered to indicate statistical significance in all statistical analyses. The agreement in ratings of AS scores obtained by two interviewers was evaluated with the kappa statistic.

A voxel-wise comparison between groups on the skeletonized NDI maps and ODI maps was conducted using the FSL randomized toolbox (permutation test [5000 permutations] using a general linear model with age, gender, and IQ as covariates of no interest). The Threshold-Free Cluster Enhancement (TFCE) method was used for multiple comparisons correction. $P < 0.05$ (TFCE corrected) was used as the significance level. To facilitate visualization, the raw statistical images were further processed using the TBSS fill script. The Johns Hopkins University ICBM-DTI-81 White-Matter Labels atlas was used as a reference to identify WM tracts that showed significant differences between groups.

After the voxel-wise comparison, NDI and ODI values extracted from the WM cluster showed significant differences between groups. Spearman's correlation analyses were further performed to compare the AS score with the mean NDI and ODI values of these clusters within the

Table 1
Demographics data of study participants.

	PNE participants (n = 29)	Control participants (n = 34)	Chi-square, t or U value	P value
Age	9.8 (1.2)	10.3 (1.6)	1.382	0.17
Sex (% male)	16 (59%)	19 (56%)	0.0032	0.95
Years of education	4.8 (1.0)	4.9 (0.9)	0.42	0.68
AS scores	5 (4–6)	4 (2–5)	330	0.02*
VIQ	104 (9.3)	104 (9.7)	0.0	0.99
PIQ	106 (10.1)	107 (10.6)	0.38	0.70
FIQ	105 (9.6)	106 (10.3)	0.39	0.69

Note: Data are presented as median (IQR), frequency (%), or mean (SD).
  * $P < 0.05$

PNE group. $P < 0.05$ was considered to indicate statistical significance.

3. Results

Three children with PNE and two children in the control group failed to complete NODDI image acquisition, so data for these five children were discarded. Additionally, demographic and imaging data of three children in the PNE group and three children in the control group were discarded due to obvious artifacts detected in NODDI imaging data during inspection after NODDI image acquisition of the MRI scans. The data of 63 subjects (29 children in the PNE group and 34 children in the control group) were included in the current study.

Participant demographics are presented in Table 1. Age and sex were matched between controls (age = 10.3 ± 1.6 years; 56% males) and children with PNE (age = 9.8 ± 1.2 years; 59% males). The FIQ, VIQ, and PIQ values did not differ between the two groups. Inter-observer agreement in AS scores of all participants between two interviewers was significant (at 0.91 with the *Kappa* statistic), suggesting reproducible results.

Compared with the control group, children with PNE had lower ODIs in WM fiber tracts of the bilateral superior longitudinal fasciculus (SLF) and higher ODIs in the bilateral internal capsule (IC) and right anterior thalamic radiation (ATR) than controls ($P < 0.05$, TFCE corrected). PNE children also had lower NDIs in the bilateral IC and the cingulum and higher NDIs in the bilateral SLF ($P < 0.05$, TFCE corrected; Fig. 1, Table 2). The NDI value of the right ATR showed a significant negative correlation with AS scores in the PNE group ($r = -0.842$, $P < 0.001$; $r = -0.780$, $P < 0.001$; Fig. 2**A-B**).

4. Discussion

In the current study we assessed WM microstructural abnormalities in children with PNE using NODDI technology. Lei et al.'s (Lei et al., 2012c) previous DTI study (using an SPM-based voxel-wise group analysis method) revealed a decrease in FA within multiple gray matter abnormalities in PNE children; however, given our study focused on WM, we performed group analysis using the TBSS method, which has been proved to be more sensitive to detect WM changes than SPM (Focke et al., 2008). As a result, our group comparison was confined within the FA skeleton and the gray voxels were excluded. To the best of our knowledge, this is the first study of microstructural measurement involving WM tracts in children with PNE using the NODDI technique. Differences of neurite orientation dispersion and/or density in WM fiber tracts of the SLF, IC, ATR, and cingulum existed between children with PNE and controls.

With NODDI technology we can depict the components (intra- and extraneurite) and geometric organization (dispersion level) of the WM microstructure. A previous study suggested that the NDI is a marker of WM maturation in childhood and adolescence (Genc et al., 2017). However, the ODI values of WM increase following an exponential pattern (Chang et al., 2015), and are relatively stable during late childhood and early adolescence (Mah et al., 2017); furthermore, the ODI values vary in different regions and are related to multiple neurobiological processes, including fanning of axons, fiber crossing, glial infiltration, and neurite pruning (Batalle et al., 2017). Therefore, we had to evaluate the microstructural abnormalities of WM in PNE children according to the differences in both NDI and ODI values (Genc et al., 2017).

The bilateral IC of children with PNE had higher ODIs and lower NDI values than the bilateral IC of healthy controls. We speculate that the lower NDI values may result from delayed neural maturation; due to the lower neurite density, the neurites may be less coherently organized and tend to be scattered. Given that the sensory afferent signal of bladder filling is projected to the cortical area through the IC, we speculate that abnormally matured WM of the IC may inhibit the relay of sensory afferent information from the bladder to the cerebral cortex. Hence, the altered microstructure of the IC may result in the inability to wake up from sleep in response to the need to urinate in children with PNE.

The ATR also showed decreased NDI values, which may also be due to the late development of non-myelinated WM fibers within the ATR. These findings were consistent with the structural and functional abnormalities within the frontal lobe and the weakened functional connectivities between the thalamus and frontal lobe that were suggested in a previous neuroimaging study (Yu et al., 2013, 2020). The thalamus plays a role in sensory gating and consciousness switching. The frontal lobe also plays a key role in the process of waking up and maintenance of consciousness. Previous MRI studies have suggested that the changes in functional connectivity between the thalamus and frontal lobe result in cortical arousal. Therefore, the lower NDI value of the ATR, which connects the thalamus and the frontal lobe, may block the transmission of arousal signals, and in turn raise the threshold of arousal. As a result, WM changes in the ATR may make it difficult for children with PNE to wake up from sleep and render them more susceptible to enuresis. In
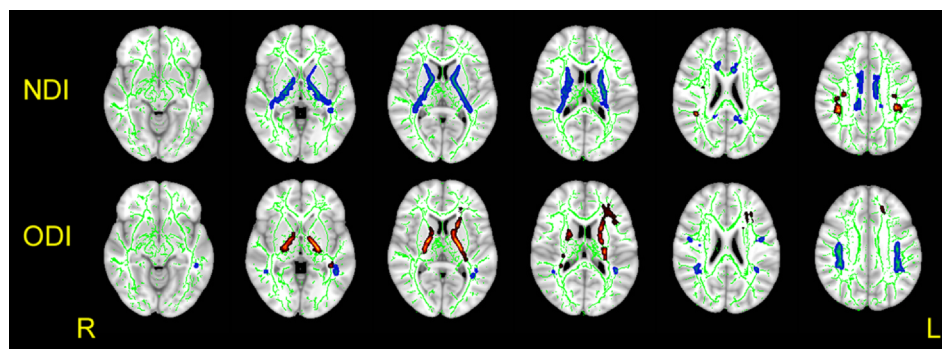

Fig. 1. Comparison of NDI and ODI values between children with PNE and controls. Compared with the control group, children with PNE had lower ODIs in WM fiber tracts of the bilateral superior longitudinal fasciculus (SLF) (blue, upper line) and higher ODIs in the bilateral internal capsule (IC) and the right anterior thalamic radiation (ATR) than controls ($P < 0.05$, TFCE corrected) (red, lower line). PNE children also had lower NDIs in the bilateral IC and the cingulum (blue, upper line) and higher NDIs in the bilateral SLF (red, upper line) ($P < 0.05$, TFCE corrected). (For interpretation of the references to colour in this figure legend, the reader is referred to the web version of this article.)

Table 2
Suprathreshold clusters for the comparison between groups ($P < 0.05$, TFCE corrected).

Cluster	Voxels	P value	MNI coordinates			Side	Anatomic Location
			X (mm)	Y (mm)	Z (mm)		
NDI PNE < control							
	419	0.024	11	−2	31	Right	Cingulum
	222	0.027	−7	−10	33	Left	
	2183	0.016	20	−6	8	Right	Internal capsule
	1963	0.011	−14	8	6	Left	
NDI PNE > control							
	232	0.037	39	−35	31	Right	Superior longitudinal fasciculus
	117	0.010	−34	−36	34	Left	
ODI PNE > control							
	845	0.033	−33	23	20	Left	Anterior thalamic radiation
	1062	0.022	−19	−10	2	Left	Internal capsule
	508	0.035	20	−16	−1	Right	
ODI PNE < control							
	694	0.041	40	−20	31	Right	Superior longitudinal fasciculus
	580	0.032	−37	−39	29	Left	

addition, the thalamo-frontal neural circuit also takes part in the cognitive process of attention; therefore, the microstructural abnormalities of the ATR may also be related to attention deficits discovered by previous studies (Yu et al., 2013).

However, the intracerebral fibers of the SLF and the cingulum in children with PNE showed increased NDI values, which indicated that the extent of myelination or pruning of axons in the SLF and cingulum may be higher in children with PNE than in controls. In addition, the SLF had decreased ODIs. Therefore, we speculate that the dispersion of neurite orientation may be limited by the larger volume of neurites.

The microstructural changes in the SLF and cingulum may enhance structural connectivity. The changes in the SLF may enhance the connectivity between the frontal and parietal cortices to compensate for the declined projection to the parietal and prefrontal lobes through the IC (Schmahmann et al., 2007). The changes in the cingulum may enhance the connectivity within the default mode network (DMN) (van den Heuvel et al., 2008), which involves monitoring and regulating the conscious state. Given that structural and functional deficits have been reported in PNE children in some studies, we speculate that this enhanced connectivity within the DMN may be a compensation for the declined projection to the prefrontal lobes through the ATR.

The abnormalities of NODDI metrics demonstrated in the current study provide evidence which supports the microstructural abnormalities of WM in children with PNE. Nevertheless, we wish to point out a

few limitations of our study. First, the limited sample size and the cross-sectional design of the current study limited our ability to validate the conclusions and examine the temporal dynamic changes with respect to the neural development in children with PNE. Therefore, our initial results require further studies including more diverse cohorts. Second, NODDI remains a model for estimating the microstructure, and NODDI parameters, such as NDI and ODI, are still phenomenological. Further studies are necessary to assess the accuracy of the NODDI model in estimating neurite structure. Third, although a previous study has suggested that the AS scores of PNE children were higher than those of controls (Chandra et al., 2004), the AS score only reflects a general arousal problem, and is not specific to the difficulty of waking up from the sensation of a full bladder, which must be considered when reviewing our results. More clinical data could have been included to further investigate the relationship between abnormal MRI findings and symptoms of enuresis.

5. Conclusion

In conclusion, we have demonstrated the abnormalities in the WM fiber tract microstructure of the SLF, IC, ATR, and cingulum in children suffering from PNE. Our study provided evidence for an altered WM microstructure in PNE children and a potential relationship between WM and AS measures, which warrants future multivariate analyses
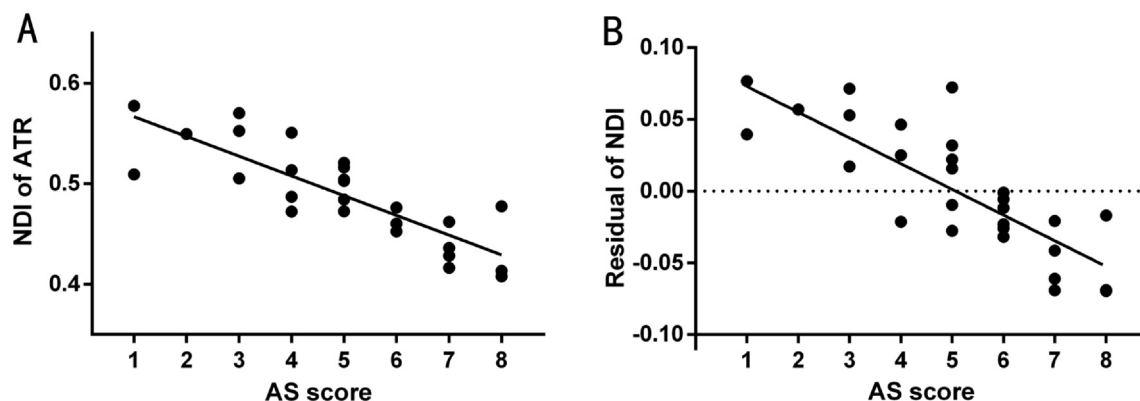

Fig. 2. Relationship between NODDI parameters and clinical data in the PNE group. (A) The NDI value of the right ATR showed a significant negative correlation with AS scores ($r = -0.842$, $P < 0.001$). (B) The fitted NDIs value of the right ATR showed a significant negative correlation with AS scores ($r = -0.780$, $P < 0.001$). The fitted values indicate the residuals of the original values of the NDI value of the left IC after correcting for age, gender, FIQ, and years of education.

with appropriate sample sizes. Importantly, our findings support the need for intensive investigation for altered WM microstructures in PNE children.

CRediT authorship contribution statement

Hongbin Sun: Conceptualization, Methodology, Software. **Bing Xue:** Visualization, Investigation. **Miao Peng:** Writing - review & editing. **Hongwei Ma:** Conceptualization, Validation. **Bing Yu:** Data curation, Writing - original draft. **Yang Hou:** Writing - review & editing. **Qiyong Guo:** Supervision.

Declaration of Competing Interest

The authors declare that they have no known competing financial interests or personal relationships that could have appeared to influence the work reported in this paper.

Acknowledgments

Appendix A. Supplementary data

Supplementary data to this article can be found online at https://doi.org/10.1016/j.nicl.2020.102389.

References

Batalle, D., Hughes, E.J., Zhang, H., Tournier, J.-D., Tusor, N., Aljabar, P., Wali, L., Alexander, D.C., Hajnal, J.V., Nosarti, C., Edwards, A.D., Counsell, S.J., 2017. Early development of structural networks and the impact of prematurity on brain connectivity. NeuroImage 149, 379–392.

Billiet, T., Mädler, B., D'Arco, F., Peeters, R., Deprez, S., Plasschaert, E., Leemans, A., Zhang, H., den Bergh, B.V., Vandenbulcke, M., Legius, E., Sunaert, S., Emsell, L., 2014. Characterizing the microstructural basis of "unidentified bright objects" in neurofibromatosis type 1: a combined in vivo multicomponent T2 relaxation and multi-shell diffusion MRI analysis. NeuroImage: Clinical 4, 649–658.

Chandra, Manju, Saharia, Reeta, Hill, Vanessa, Shi, Qiuhu, 2004. Prevalence of diurnal voiding symptoms and difficult arousal from sleep in children with nocturnal enuresis. J. Urol. 172 (1), 311–316.

Chang, Y.S., Owen, J.P., Pojman, N.J., Thieu, T., Bukshpun, P., Wakahiro, M.L., Berman, J.I., Roberts, T.P., Nagarajan, S.S., Sherr, E.H., Mukherjee, P., 2015. White matter changes of neurite density and fiber orientation dispersion during human brain maturation. PLoS One 10, e0123656.

Focke, N.K., Yogarajah, M., Bonelli, S.B., Bartlett, P.A., Symms, M.R., Duncan, J.S., 2008. Voxel-based diffusion tensor imaging in patients with mesial temporal lobe epilepsy and hippocampal sclerosis. NeuroImage 40 (2), 728–737.

Genc, S., Malpas, C.B., Holland, S.K., Beare, R., Silk, T.J., 2017. Neurite density index is sensitive to age related differences in the developing brain. NeuroImage 148, 373–380.

Jelescu, I.O., Veraart, J., Adisetiyo, V., Milla, S.S., Novikov, D.S., Fieremans, E., 2015. One diffusion acquisition and different white matter models: how does microstructure change in human early development based on WMTI and NODDI? NeuroImage 107, 242–256.

Lei, D., Ma, J., Du, X., Shen, G., Tian, M., Li, G., 2012a. Altered brain activation during response inhibition in children with primary nocturnal enuresis: an fMRI study. Hum. Brain Mapp. 33 (12), 2913–2919.

Lei, D.u., Ma, J., Du, X., Shen, G., Tian, M., Li, G., 2012b. Spontaneous brain activity changes in children with primary monosymptomatic nocturnal enuresis: a resting-state fMRI study: brain activity changes in children with PMNE. Neurourol. Urodyn. 31 (1), 99–104.

Lei, D., Ma, J., Shen, X., Du, X., Shen, G., Liu, W., Yan, X., Li, G., 2012c. Changes in the brain microstructure of children with primary monosymptomatic nocturnal enuresis: a diffusion tensor imaging study. PLoS One 7, e31023.

Lei, D.u., Ma, J., Zhang, J., Wang, M., Zhang, K., Chen, F., Suo, X., Gong, Q., Du, X., 2015. Connectome-scale assessments of functional connectivity in children with primary monosymptomatic nocturnal enuresis. Biomed Res. Int. 2015, 1–8.

Mah, A., Geeraert, B., Lebel, C., 2017. Detailing neuroanatomical development in late childhood and early adolescence using NODDI. PLoS One 12, e0182340.

Nevéus, T., von Gontard, A., Hoebeke, P., Hjälmås, K., Bauer, S., Bower, W., Jørgensen, T.M., Rittig, S., Walle, J.V., Yeung, C.-K., Djurhuus, J.C., 2006. The standardization of terminology of lower urinary tract function in children and adolescents: report from the standardisation committee of the international children's continence society. J. Urol. 176 (1), 314–324.

Schmahmann, J.D., Pandya, D.N., Wang, R., Dai, G., D'Arceuil, H.E., de Crespigny, A.J., Wedeen, V.J., 2007. Association fibre pathways of the brain: parallel observations from diffusion spectrum imaging and autoradiography. Brain 130 (3), 630–653.

Smith, S.M., Jenkinson, M., Johansen-Berg, H., Rueckert, D., Nichols, T.E., Mackay, C.E., Watkins, K.E., Ciccarelli, O., Cader, M.Z., Matthews, P.M., Behrens, T.E.J., 2006. Tract-based spatial statistics: Voxelwise analysis of multi-subject diffusion data. NeuroImage 31 (4), 1487–1505.

van den Heuvel, M., Mandl, R., Luigjes, J., Hulshoff Pol, H., 2008. Microstructural organization of the cingulum tract and the level of default mode functional connectivity. J. Neurosci. 28 (43), 10844–10851.

Wang, M., Zhang, K., Zhang, J., Dong, G., Zhang, H., Du, X., 2015. Abnormal Neural Responses to Emotional Stimuli but Not Go/NoGo and Stroop Tasks in Adults with a History of Childhood Nocturnal Enuresis. PLoS One 10, e0142957.

Xu, J., Moeller, S., Auerbach, E.J., Strupp, J., Smith, S.M., Feinberg, D.A., Yacoub, E., Uğurbil, K., 2013. Evaluation of slice accelerations using multiband echo planar imaging at 3T. NeuroImage 83, 991–1001.

Yu, B., Guo, Q., Fan, G., Ma, H., Wang, L., Liu, N., 2011. Evaluation of working memory impairment in children with primary nocturnal enuresis: evidence from event-related functional magnetic resonance imaging. J. Paediatr. Child Health 47, 429–435.

Yu, B., Guo, Q., Liu, N., Fan, G., 2010. Evaluation of Memory/Caution Impairment in Children with Primary Nocturnal Enuresis: Evidence from Diffusion Tensor Imaging. In: RSNA 96th Scientific Assembly and Annual Meeting, Chicago.

Yu, B., Kong, F., Peng, M., Ma, H., Liu, N.a., Guo, Q., 2012. Assessment of memory/attention impairment in children with primary nocturnal enuresis: a voxel-based morphometry study. Eur. J. Radiol. 81 (12), 4119–4122.

Yu, B., Sun, H., Ma, H., Peng, M., Kong, F., Meng, F., Liu, N., Guo, Q., 2013. Aberrant whole-brain functional connectivity and intelligence structure in children with primary nocturnal enuresis. PLoS One 8, e51924.

Yu, B., Xiao, S., You, Y.i., Ma, H., Peng, M., Hou, Y., Guo, Q., 2020. Abnormal thalamic functional connectivity during light non–rapid eye movement sleep in children with primary nocturnal enuresis. J. Am. Acad. Child Adolesc. Psychiatry 59 (5), 660–670.e2.

Zhang, H., Schneider, T., Wheeler-Kingshott, C.A., Alexander, D.C., 2012. NODDI: practical in vivo neurite orientation dispersion and density imaging of the human brain. NeuroImage 61 (4), 1000–1016.